

## REPORT DOCUMENTATION PAGE

Public reporting burden for this collection of information is estimated to average 1 hour per response, including the time for reviewing the data needed, and completing and reviewing this collection of information. Send comments regarding this burden estimate or any other aspect of this collection of information, including suggestions for reducing this burden to Washington Headquarters Services, Directorate for Information Operations and Reports, 1215 Jefferson Davis Highway, Arlington, VA 22202-4302, and to the Office of Management and Budget, Paperwork Reduction Project (0704-0188), Washington, DC 20503

1. AGENCY USE ONLY (Leave blank)		2. REPORT DATE 12/29/2005		3. REPORT TYPE AND DATES COVERED 04/01/2004-09/30/2005	
4. TITLE AND SUBTITLE  Micro-Tailoring Multi-Functional Materials for Aerospace Objectives				5. FUNDING NUMBERS  FA9550-04-1-0238	
6. AUTHOR(S)  Yuri M. Shkel, Robert Rowlands					
7. PERFORMING ORGANIZATION NAME(S) AND ADDRESS(ES)  Research and Sponsored Programs      Department of Mechanical Engineering University of Wisconsin, Madison      University of Wisconsin, Madison 750 University Avenue      1513 University Avenue Madison WI 53706      Madison WI 53706				8. PERFORMING ORGANIZATION REPORT NUMBER	
9. SPONSORING / MONITORING AGENCY NAME(S) AND ADDRESS(ES)  AFOSR 875 N Randolph St. Ste 325, Rm 3112 Arlington VA 22203-1954 Dr B. Lee				10. SPONSORING / MONITORING AGENCY REPORT NUMBER	
11. SUPPLEMENTARY NOTES					
12a. DISTRIBUTION / AVAILABILITY STATEMENT  Approved for public release, distribution unlimited				20060309 067	
13. ABSTRACT (Maximum 200 Words)  This research demonstrates that both fibers and spherical inclusions in composite can be manipulated by electric or magnetic fields. This capability is applied to micro-tailor microstructure of polymeric composites to meet aerospace design objectives. Composition of graphite, glass, ceramic and metallic constituents dispersed in epoxy are considered. The ultimate goal is to achieve multifunctional performance which is superior to that of conventional composites. This includes controlling local orthotropy, as well as developing self-sensing and health monitoring capabilities. The developed computational optimization procedure demonstrates that stress concentrations in perforated composites can be significantly reduced by appropriately orientating the fibers in the neighborhood of the discontinuities. Considerable progress has also been made towards implementing these features when manufacturing real components. Novel capacitive sensors have been developed which can measure a component's strains without being bonded to the component. These sensors can be orientated arbitrarily and still provide both the magnitude and directions of the principal strains and stresses.					
14. SUBJECT TERMS				15. NUMBER OF PAGES 21	
				16. PRICE CODE	
17. SECURITY CLASSIFICATION OF REPORT	18. SECURITY CLASSIFICATION OF THIS PAGE	19. SECURITY CLASSIFICATION OF ABSTRACT	20. LIMITATION OF ABSTRACT		

## OBJECTIVES AND ACHIEVEMENTS

The initial objectives of this three year project were to advance the novel manufacturing paradigm that the microstructure of polymeric composites can be micro-tailored during processing to meet aerospace design objectives which are not achievable using conventional composite processing methods. Since the actual funding and research time were reduced by 50%, not all of the objectives were met.

Proposed activity	Actually achieved
Substantiate the feasibility of field-aided micro-tailoring approach for processing polymeric composites suitable for aerospace applications. This includes graphite, glass, metallic and nano-clay constituents dispersed in epoxy, polyamide and polyimide.	Composites consisting of graphite, glass, ceramic and metallic constituents dispersed in epoxy were prepared and tested. Both fibers and spherical particles were manipulated by electric or magnetic field. Results demonstrate the feasibility of the technology.
Determine the mechanical, electrical and thermal responses, health monitoring and actuation capabilities of composite systems whose micro-structure has been modified.	Mechanical responses of the system having modified microstructure were tested. Self-sensing and health monitoring of acrylic specimens have been demonstrated. Components having modified micro-structure will be tested in the future. Preliminary results with piezoresistive and thermal responses were obtained but further research is necessary before submitting for publication.
Evaluate the potential of silicone rubber filled with metal or piezoelectric particles for self-sensing and actuation applications.	Silicone rubber containing either piezoelectric ( $\text{BaTi}_2\text{O}_3$ ) or carbon particles was tested and the dielectrostriction and piezoresistive responses measured.
Assess whether field-aided technology can increase self-sensing and actuation capabilities.	Our preliminary study (outside this proposal) indicate the potential of micro-tailoring to increase self-sensing and actuation capabilities. However, we had inadequate time to explore this direction in sufficient detail.
Demonstrate that micro-tailoring the material in the neighborhood of geometric discontinuities in loaded composites can decrease stress concentration and thereby reduce the amount of material required to provide desired component strength.	Our computational results to date substantiate the enhanced performance of parts having locally varying orthotropy. We have made considerable progress towards implementing these features in real components. However experimental validation of the obtained results requires further research.
Show that by synergizing both engineered component design and design of the material can (a) reduce stress concentrations, (b) provide self-sensing and actuation capabilities, (c) control hydrothermal and residual stresses and (d) create desirable thermal and electrical responses.	We have made substantial progress towards understanding relationship between most of the listed functions. However, there was insufficient time to adequately study combined multifunctional response.

### FIELD-AIDED MICRO-TAILORING (FAiMTa) TECHNOLOGY

The authors have recently developed a process which uses an electric field to locally modify the distribution and orientation of inclusions in polymers. Functionally graded composites manufactured by this novel technology, called field-aided micro-tailoring (FAiMTa), are free of many shortcomings associated with traditional manufacturing techniques [1-4]. Electrically-induced forces acting on inclusions exceed those in centrifugal processes or during in-mold flows. Furthermore, these electric forces can be applied locally and in desirable directions. Required times for electric field exposure are an order of seconds, which enables the FAiMTa process to be used with continuously fabricated materials.

The essence of the Field-Aided Micro-Tailoring (FAiMTa) technology is curing, in the presence of an electric field, a liquid polymer containing randomly dispersed micro or nano-sized particles, fibers or platelets. Upon curing, the resulting solid composite has a microstructure aligned with the applied electric field. Either an AC or DC field can be used to assemble, rearrange and orient organic and inorganic particles whose electric properties (conductivity, dielectric, etc.) differ from those of the suspending medium. Moreover, the frequency of the applied electric field can be chosen such that virtually any inclusion can be manipulated in any liquid. Traditional composites have a fixed effective fiber content and orientation throughout a component. On the other hand, FAiMTa enables forming fiber-like chains of spherical particles of desired orientation and effective volume content in desired regions of an engineered component. Similarly, an applied electric field orients non-spherical inclusions such as fibers or disk-like nano-clay particles. Several mechanisms influence the redistribution of inclusions. Dipole-dipole attraction produces chain-like structure ("pseudo-fibers") of polarized inclusions which provides mechanical and electric orthotropy in the resulting solid composite. Similarly, torque acting on flake- or fiber- like inclusions orients the inclusions in desirable directions Figure 1. Rheological aspects of the FAiMTa technology have been previously examined [3].

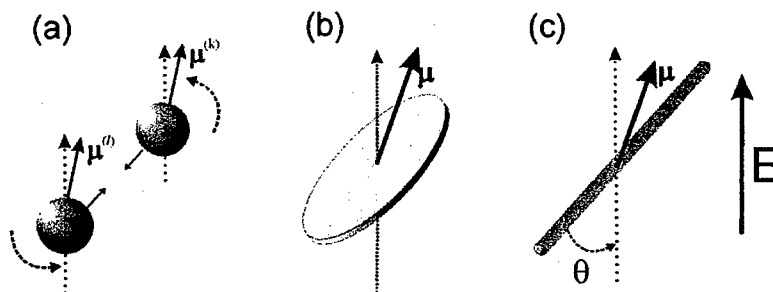


Figure 1: (a) Dipole-dipole attraction between two inclusions, (b) torque acting on a flake and (c) torque acting on a fiber.  $\mu$  represents electric field-induced polarization (Ref. [3]).

The times of Table 1 are verified by direct microscopic observations of test specimens during the alignment process [3]. The short processing times illustrate that the FAiMTa technique provides a practical method for manufacturing orthotropic composite materials having locally controlled fiber orientation.

Materials	Viscosity (Poise)	Processing Times	
		10 kV/mm	1 kV/mm
Low Density Polyethylene	3160	3 sec	300 sec
Polypropylene	10000	10 sec	1020 sec
Polycarbonate	3160	3 sec	300 sec
Polyamide (Nylon)	700	0.7 sec	66 sec
Poly(ethylene terephthalate)	1000	1 sec	96 sec
Epoxy with Hardener	0.7	0.007 sec	0.7 sec

Table 1: Time to align particles in common matrix materials (Ref. [3])

### FEASIBILITY OF THE FAiMTa TECHNOLOGY

Figure 2 shows that graphite powder, originally randomly dispersed in epoxy, has been oriented by an AC electric field. The orthotropy of the material in this figure is controlled by the electrode configuration. Graphite chains, which are in the material's thickness direction, are produced by parallel-plate electrodes, Figure 2 (a). Chains are formed parallel to the surface by interdigitated electrodes, Figure 2 (b). The depth of the particle arrangement of Figure 2 (b) is controlled by the distance between the electrodes and the amplitude of the applied field. The structures in Figure 2 were obtained using a 1 kV/mm field which was generated by applying a 2.5 kV voltage over a 2.5 mm gap between the electrodes. The same field can be readily obtained over a 25 mm gap using readily available 25 kV voltage source. The dielectric strength of the epoxy is in the range of 14 kV/mm to 20 kV/mm, which is well above the magnitude used for FAiMTa technology.

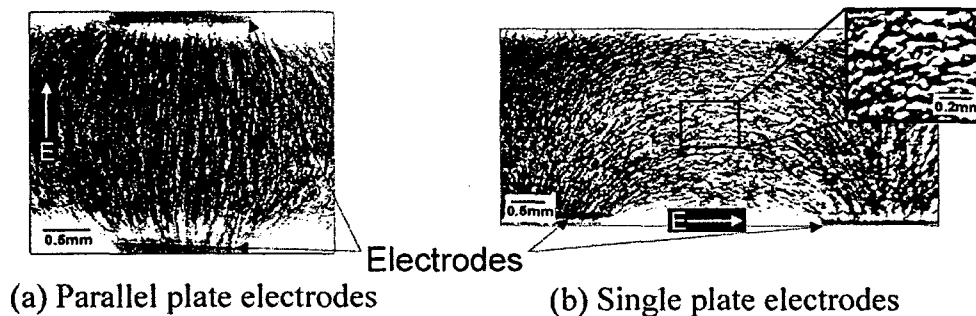
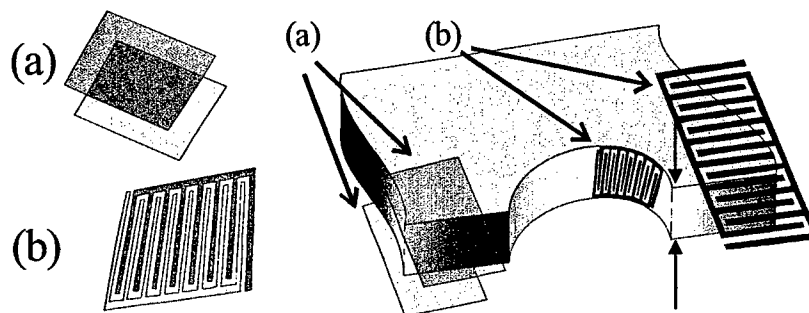


Figure 2. Material's orthotropy is controlled by the configuration of electrodes: (a) parallel-plate electrodes produce chains oriented through the thickness of the material; (b) planar electrodes form chains oriented in the in-plane direction.

Figure 3 outlines the paradigm of the FAiMTa technology in modifying the internal microstructure of a polymeric composite during its fabrication to achieve a design objective. A combination of parallel plate and interdigitated electrodes can be positioned on the mold surfaces. By selecting frequency, direction and magnitude of the electric field, inclusions of any composition and shape can be rearranged within the material to achieve desired structure. The

obtained structure is preserved by curing it in the presence of the electric field. This concept is the cornerstone for fabricating solid composite materials having space varying material orthotropy.



**Figure 3. Electrode configurations which can be employed to modify the structure: (a) parallel-plate electrodes create orthotropy in the perpendicular-to-plane direction, and (b) planar interdigitated electrodes produce in-plane orthotropy.**

#### **Materials and Sample Preparation**

The ceramic particles (Zeeosphere™ Ceramic Microspheres from 3M Corp.) and graphite particles (West System 423) have an average diameter of 6  $\mu\text{m}$  and a maximum diameter of 40  $\mu\text{m}$ . The epoxy resin (West System-105), curing agent (West System-206) and glass fibers were obtained from Gougeon Brothers, Inc. The round glass fibers have an average diameter of 2.5  $\mu\text{m}$ . All micro composite specimens contain 5, 10, 20 or 40 vol.% inclusions in epoxy. The nanoclay/polyamide (nylon-6) composite was obtained from the RTP Company.

Figure 4 illustrates the electrode configuration used to align inclusions in epoxy. During curing, an electric field having 1.2 ~ 2.4 kV/mm strength and 5 Hz frequency was applied. Orthotropic specimens were prepared having their structure oriented in the tensile/compression (parallel, ||) or transverse (perpendicular,  $\perp$ ) directions, Figure 4 (a) and (b), respectively. Specimens cut parallel to the electrodes have transverse orientation of orthotropy while specimens cut perpendicular to the electrodes have longitudinal orientation of orthotropy. All specimens were approximately 10mm $\times$ 1.5mm (W $\times$ T) with a cantilever length of 17mm. Response of the orthotropic samples was compared with samples having similar composition but random structure as shown in Figure 4(c). Micrographs of the composite structures are shown in Figure 5. Initially randomly dispersed ceramic particles are aligned by applying the electric field to form chains of particles, Figure 5(a). The applied electric field similarly orients glass fibers in epoxy as shown in Figure 5(b).

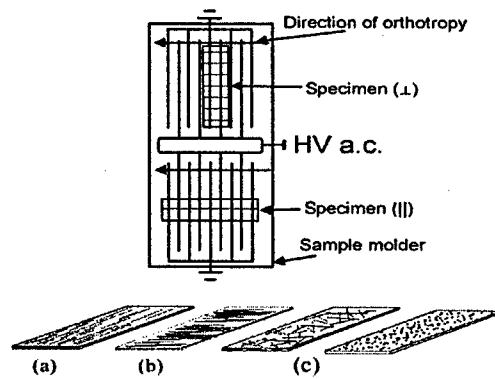


**Figure 4:** Fabricated specimens have fibers (a) parallel (||) and (b) perpendicular (⊥) to their longitudinal axis. (c) Random structure is produced without an applied field.

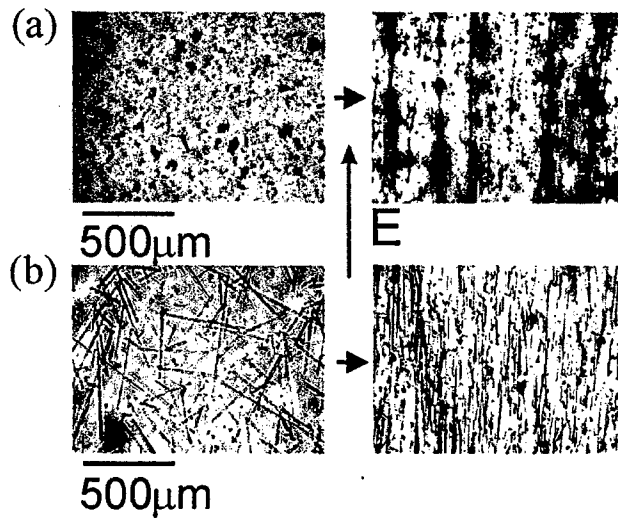


**Figure 5:** Alignment by electric field of initially isotropic composites: (a) ceramic particles, and (b) glass fibers in epoxy (Ref. [6])

### Characterization of Field-Tailored Composites

Ceramic and glass-fiber composites were tested using a dynamic mechanical analyzer DMA-2980 from TA Instruments. The cantilever beam specimens were cycled at 10 Hz with an end amplitude of 10  $\mu\text{m}$  at a constant temperature of 30°C. Measured elastic moduli of orthotropic specimens oriented parallel (||), and perpendicular (⊥), to the cantilever length are compared with those of the randomly oriented specimens having similar composition. The glass-fiber and ceramic composites demonstrate similar behavior. Figure 6 shows the normalized moduli of respective isotropic,  $E_r$ , and orthotropic ceramic/epoxy and glass-fiber/epoxy composites as a function of volume content. Figure 6(a) demonstrates the relation for ceramic powder in an epoxy matrix and Figure 6(b) is similar to that for the glass-fiber/epoxy composites. For the

structure oriented in the parallel direction ( $\parallel$ ), both systems have storage moduli 15 to 20% higher than that of their corresponding random samples. Similarly, inclusions oriented in the perpendicular direction ( $\perp$ ) decrease the elastic modulus by 15 to 20% below their isotropic counterpart. This shows that composites having oriented chains of ceramic particles behave similarly to glass-fiber composites.

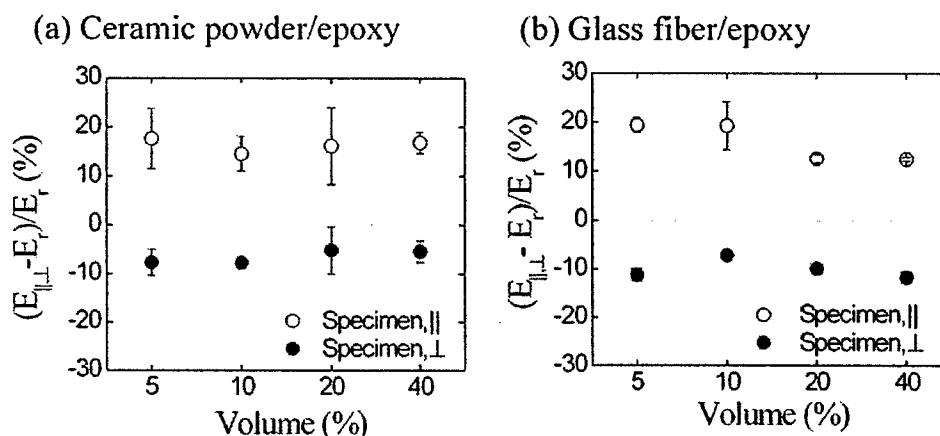


Figure 6 Measured moduli of (a) ceramic powder/epoxy and (b) glass fiber/epoxy composites fabricated by FAiMTA conditions,  $E = 1.2\text{ kV/mm}$  and  $f = 5\text{ Hz}$ .

### HOLY GRAIL: COMPOSITES WITH LOCALLY VARYING ORTHOTROPY

There are a number of ways in which one can reduce stress concentrations in a notched or perforated composite members. For example, stacking sequences, number of plies, fiber directions, etc. can be parameters for optimization. The problem is complicated by the difficulties of defining object functions and the complexity of design spaces. A circularly-perforated tensile plate is a prevalent engineering component. The stress concentration factor for an infinite isotropic configuration is three [5]. The maximum stress concentration occurs at the hole perimeter  $90^\circ$  from the loading direction. A focus of this study is to appropriately orient the fibers in perforated orthotropic composite plates. The ultimate goal is to control the local structural stiffness so as to minimize the stress concentration at the hole. Previous design philosophies for reducing the tensile stress concentration in composite plates with a hole are based on the idea of using curvilinear fiber directions aligned in a particular direction such as the stress flow or fluid stream lines. Several methods have been investigated for this purpose. They include modifying the hole shape to minimize stress concentration [6] as well as changing the stiffness of the region near the hole [7, 8].

### Numerical optimization

Katz [9] and Hyer [8] used sequential linear programming to increase buckling resistance and strength of a panel through optimization of the fiber directions. Hyer and Charette utilized sensitivity analysis and gradient search techniques [8, 10] to rearrange fiber directions in a uniaxially loaded laminated plate containing a circular hole. Fibers aligned with the principal

stresses in the plate substantially increased the strength. Hermanson [7] reduced the tensile stress concentration by implementing stream lines of fluid around a circular hole as the fiber directions.

We minimized the tensile stress concentration at a round hole in a composite by synergizing FEA and optimization numerical modules. The geometry of the model was divided into discrete finite elements. The design variables were defined to be the fiber directions of each element. The number of design variables was therefore the same as the total number of the elements. It is assumed that a large amount of design variables would be an obstacle for the optimization process when approaching the optimum value. The developed code is a fully integrated finite-element solver and structural optimization system. The optimization of fiber direction is implemented using the feasible direction parallel optimization algorithm and includes a FEA sub-module. It is a basic method developed for constrained nonlinear optimization problems. Figure 7 outlines the optimization procedure. The main optimization process integrates optimization objectives with the FEA. For every iteration loop, the process designates design variables, the fiber directions of each element, to the FEA module. The FEA module uses the information to establish the stiffness matrix. After the FEA module calculates the displacements, strains and stresses and achieves convergence, the resultant values are returned to the main process.

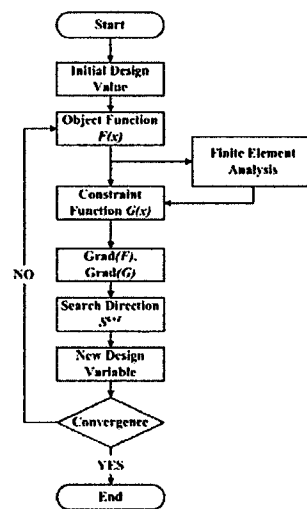


Figure 7: Schematic diagram of optimization with parallel FEA module

The optimum solution at a certain time is then used to update the stiffness of the finite elements and a new finite element analysis is performed. This entire process is repeated until an optimum solution is reached. Large complex problems having many design variables can be optimized in this way. Prior studies of the optimization of composite structures have been accomplished; however previous approaches allow optimization when stresses are known analytically. It does not seem that such analytic stresses can be immediately implemented into a finite element program. On the other hand, the present parallel algorithm describes, develops and applies an optimization procedure which can perform within a finite element program.



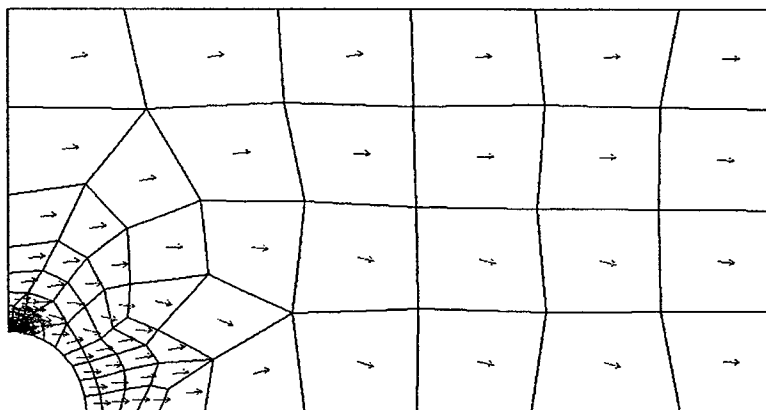


Figure 8: Optimized fiber direction

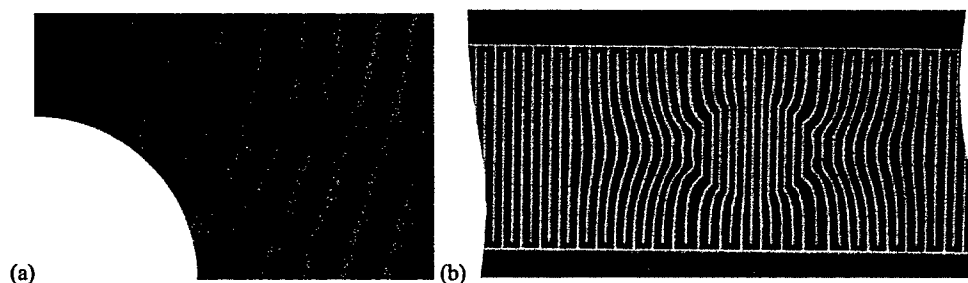


Figure 9: (a) Chains of carbon particles are oriented around a hole for reduction of stress concentration; (b) Electrode geometry used to create the pattern.

### Optimization results

Results from this study are represented in Figure 8. The numerical optimization technique used here gives a predicted stress concentration factor of only 1.52 which is a very significant improvement over other methods. Prior results based on stream-line fiber orientation obtained a stress concentration factor of 3.69 and the principal-stress fiber orientation technique had a factor of 4.04. The integrated numerical optimization procedure has been theoretically shown to be highly effective [11].

### ***FAiMTa: A TECHNOLOGICAL BREAKTHROUGH?***

The thrust of the FAiMTa process is to align the inclusions in predefined directions. Following the just-described numerical analysis the objective could be to physically implement optimal fiber orientation and to achieve this reduced stress concentration. Figure 9(a) shows the orientation of carbon particles around a circular hole and Figure 9(b) as well as the electrode geometry used to create the microstructure in Figure 9. The sample was cured at room temperature under an applied electric field of 2000V/mm and a frequency of 50Hz. The white bands in Figure 9 are due to the movement of particles away from the electrodes and can be

eliminated by better electrode design and improving the field-exposure regime. Figure 10 demonstrates the feasibility of the FAiMTa process for locally optimizing the internal microstructure of the composite to achieve the desired objective in material design, e.g., to reduce stress concentration at the hole.

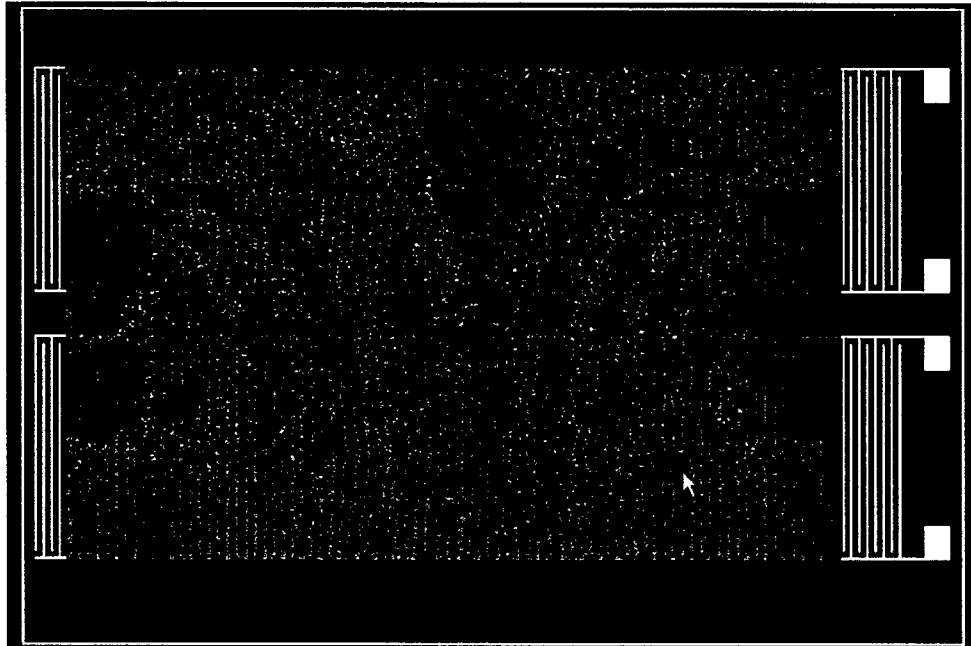


**Figure 10: Speckle testing of the nano-carbon composite plate having modified and unmodified areas: upper part of the image corresponds to the area which has been modified using the electrode pattern shown in Figure 9(b), lower part of the image has random distribution of inclusions. Electrode grid is over imposed for convenience.**

### **MULTIFUNCTIONAL MATERIALS FOR SELF-SENSING**

This preliminary study is laying the foundation for self-powered sensors embedded in load-bearing structures. The approach would synergize three technologies: (1) a dielectrostriction sensing technique to monitor strains, stresses and structural integrity (locally or full-field) in composites without relying on mechanical contact (addressed below), (2) energy harvesting using piezoelectric materials and novel electro-active composites (not addressed in this study), and (3) field-aided technology, which employs electromagnetic fields to locally modify the structure of multifunctional nanocomposites. The goals are to advance the fundamental knowledge for design and manufacturing of self-powered sensor systems, and develop and demonstrate prototype devices. Anticipated outcomes of this research include autonomous, self-powered and easily-mounted sensor systems for health-monitoring load-bearing structures.

**Strains/stresses and structural integrity sensing** utilizes dielectrostriction in composite materials. The sensor measures the dielectrostriction response of either the load-bearing structure (self-sensing) or a functionally-graded interface material. Dielectrostriction is selected because such sensors dissipate little or no energy – a significant advantage in energy-limited applications. Such sensors are easier to manufacture and assemble than are traditional strain gages. Professor Shkel holds a U.S. Patent on this sensing technology [12]. **Three types of prototype sensor packaging** are proposed: (1) attached sensors exploiting self-sensing abilities of the structure, (2) sensors embedded within the load-bearing structure, and (3) sensors interfacing functionally-graded composites to monitor metal load-bearing structures.

### Dielectrostriction Sensing

A fundamental property of any dielectric material is the linear variation of the dielectric properties with deformation [12-25]. This dielectrostriction phenomenon resembles the well-known photoelastic effect, which is used for full-field stress monitoring of transparent materials. The photoelastic effect can be considered as a manifestation of dielectrostriction in the optical range of the electromagnetic spectrum. However, while optical measurements are limited to the transparent materials, dielectrostriction is applicable to both transparent and opaque materials. Dielectrostriction measurements constitute a new and novel approach to study strains and stresses in various structures. Potential applications of dielectrostriction include stand-alone sensors, in-line material health monitoring of structures, as well as multifunctional smart materials with self-sensing and actuating capabilities. We have preliminary results for preparing and utilizing a planar capacitor sensor rosette to measure the dielectrostriction response. This sensor, which monitors material deformation of the substrate without contacting it mechanically, confirms the linearity of the dielectrostriction response with strains and stresses.

### Monitoring Dielectrostriction

The technique uses set of interdigitated electrodes deposited on a rigid substrate. Such a planar-capacitor sensor is located in close proximity to (but not in a contact with) a monitored dielectric material and does not constrain the mechanical deformations of the member. The capacitance,  $C_\theta$ , of the sensor is  $C = Q/V$ , where  $Q$  is the total charge of the electrodes and  $V$  is the potential difference. The dielectric tensor,  $\epsilon$ , of an anisotropic material has only three diagonal components  $\epsilon_1$ ,  $\epsilon_2$  and  $\epsilon_3$  in the principal coordinate system,  $x_1x_2x_3$ , Figure 11. The electrodes are located in  $x_1x_2$ -plane and form an arbitrary angle,  $\theta$ , with the principal axis,  $x_2$ , of the dielectric material. The sensor capacitance is expressed as [18, 19, 21]

$$C_\theta = \frac{Q}{V} = C_0 (\epsilon'_{eff} + \epsilon''_{eff}), \quad C_0 = \frac{\epsilon_0 L \ln 2}{\pi}, \quad (1)$$

$$\epsilon'_{eff} = \epsilon''_{eff} = \sqrt{\epsilon_3 \left[ \left( \frac{\epsilon_1 + \epsilon_2}{2} \right) + \left( \frac{\epsilon_1 - \epsilon_2}{2} \right) \cos 2\theta \right]},$$

where  $2C_0$  is the capacitance of the electrodes in free space,  $\epsilon'_{eff}$  and  $\epsilon''_{eff}$  are the effective dielectric constants of a material on the top and bottom of the electrodes, respectively.

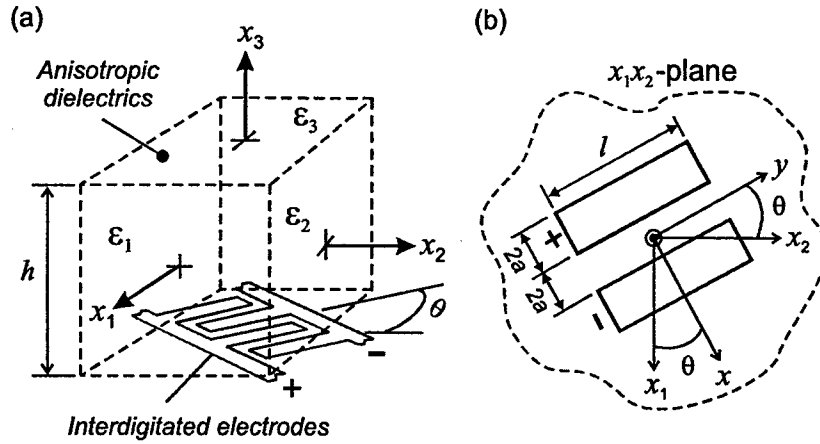


Figure 11:(a) Related to its principal coordinate system,  $x_1x_2x_3$  an anisotropic solid dielectric has three principal dielectric constants,  $\epsilon_1$ ,  $\epsilon_2$ , and  $\epsilon_3$ . Interdigitated electrodes are located in the  $x_1x_2$ -plane and form an angle,  $\theta$ , with the principal axis  $x_2$ . (b) Each electrode strip has width,  $2a$ , length,  $l$ , and is separated from the other electrodes by  $2a$ .

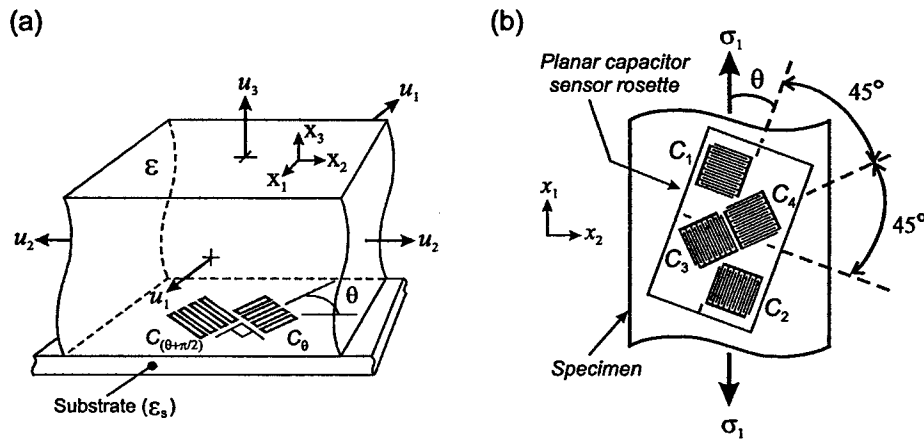


Figure 12: (a) An elastic dielectric is subjected to three-axial strains,  $u_1$ ,  $u_2$ , and  $u_3$ . Two mutually perpendicular planar capacitor sensors form angles  $\theta$  and  $(\theta+\pi/2)$  with the  $x_2$ -axis, respectively. (b) The rosette of two sets of sensors can simultaneously monitor the difference in the principal strains and the principal-strain direction.

Planar capacitor sensors such as described in Figure 11 can be utilized for strain monitoring. Consider the capacitor configuration for experimental strain analysis in Figure 12(a). Two planar capacitor sensors are located adjacent to an elastic dielectric material. The two sensors form angles  $\theta$  and  $(\theta+\pi/2)$  with the  $x_2$ -axis, respectively. The material is subjected to deformation which is described by three principal strains,  $u_1$ ,  $u_2$ , and  $u_3$ , associated with the principle coordinate system  $x_1x_2x_3$ . The difference in the capacitances of these two sensors is,

$$C_\theta - C_{\theta+\pi/2} = \frac{C_0}{2} \alpha_1 (u_1 - u_2) \cos 2\theta. \quad (2)$$

The output of such a sensor rosette is directly proportional to the difference between the two principal strains ( $u_1 - u_2$ ) and the double angle with the principal directions in the sensor plane.

Figure 12(b) shows another sensor configuration. This rosette consists of two sets of perpendicularly oriented sensors oriented at  $45^\circ$  with each other. Such a rosette is capable of separating the difference in the principal strains and the principal-strain direction. Following Eq. (2), the capacitances of each set of perpendicularly oriented sensors are

$$\begin{aligned} C_1 - C_2 &= \frac{C_0}{2} \alpha_1 (u_1 - u_2) \cos 2\theta, \\ C_3 - C_4 &= \frac{C_0}{2} \alpha_1 (u_1 - u_2) \sin 2\theta. \end{aligned} \quad (3)$$

The respective output voltages,  $V_1$  and  $V_2$ , of the capacitor bridge formed by this sensor rosette [18, 21] are

$$V_1 = K_0 (u_1 - u_2) \cos 2\theta \text{ and } V_2 = K_0 (u_1 - u_2) \sin 2\theta, \quad (4)$$

where  $K_0$  is a coefficient defined by the circuit parameters and the geometry of the sensor. This constant can be expressed as  $K_0 = \alpha_1 \omega R V_i C_0 / 2$  where  $R$  is the amplification gain,  $V_i$  and  $\omega$  are the amplitude and the frequency of input voltage to the capacitor bridge. Finally, two measurements,  $V_1$  and  $V_2$ , provide the difference of the principal strains,  $u_1 - u_2$ , and the principal strain direction,  $\theta$ ,

$$u_1 - u_2 = \frac{1}{K_0} (V_1^2 + V_2^2)^{-1/2} \text{ and } \theta = \frac{1}{2} \tan^{-1} \left( \frac{V_2}{V_1} \right). \quad (5)$$

### Experimental setup

An experimental setup for actually employing the capacitor sensors is shown in Figure 13. A set of two perpendicularly oriented planar capacitor sensors is located on (but not bonded to) the surface of a polycarbonate specimen. Resulting change in dielectric properties of the specimen is measured by the capacitor bridge circuit and conditioned by a SR830 DSP lock-in amplifier. The experimental setup in Figure 13 employing the sensor rosette of Figure 12 (b) is used to measure the principal-strain difference and the principal-strain direction. The specimen was uniaxially loaded in tension by a MTS Sintech 10/GL testing machine. The induced deformations have principal strains,  $u_1$  and  $u_2 = u_3 = -\nu u_1$ . The specimen is tested for different aligned angles of  $0^\circ$ ,  $10^\circ$ ,  $20^\circ$ , respectively and obtained values are averaged.

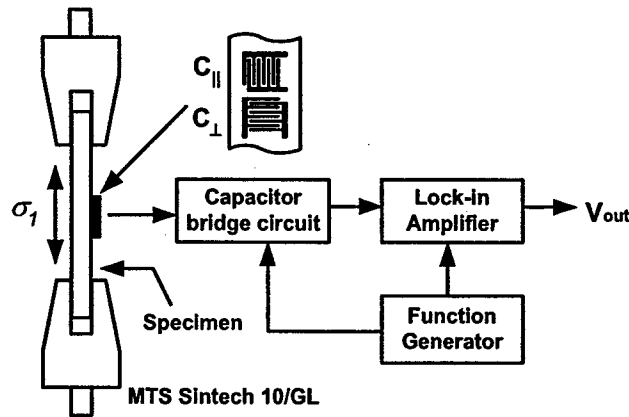
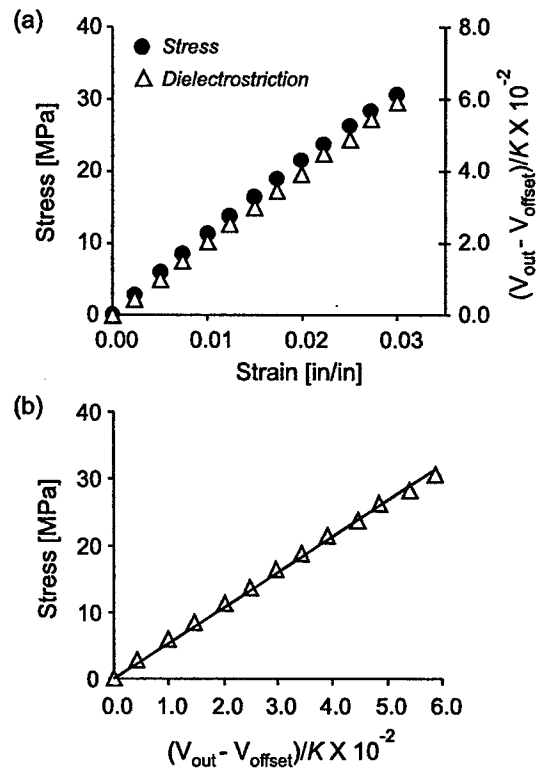


Figure 13: A sensor rosette is placed on surface of a tensile-loaded specimen. The dielectrostriction response is measured by a capacitance bridge circuit and conditioned by a lock-in amplifier.

## Results

The applied stresses and recorded strains in a polycarbonate specimen are compared in Figure 14(a). The specimen is in the linear elastic region for up to 3 % strains. The output of two perpendicularly oriented planar capacitor sensors is plotted as a function of stresses and is linear over the same range of deformations. The same data are re-plotted as the stress-dielectric response in Figure 14 (b). These experimental results illustrate the Strain-Dielectric Rule (SDR) and thereby provides the foundation for material monitoring through dielectrostriction effect.

The principal-strain difference,  $u_1 - u_2$ , and the principal directions are measured using the four-sensor rosette, and Eq. (5). Obtained results are compared to the principal-strain difference,  $u_1 - u_2 = (1 + \nu)u_1$ , with actual uniaxial longitudinal strain,  $u_1 = 0.35\%$ . Poisson ratio of an acrylic is taken in the range  $\nu = 0.35 - 0.45$ . The measurements are summarized and compared with known values in Table I. Measurements show good agreement with the applied values. Measured principal directions are within few degrees of the alignment angle. Obtained values of the principal-strain difference range from 0.33 % to 0.49 % and these are comparable to an applied value,  $(u_1 - u_2) = 0.47\% - 0.51\%$ . In this study, we used the value,  $C_0 \approx 0.7 - 0.8 \text{ pF}$ , which was measured directly using HP 4194A impedance analyzer, to calculate the principal-strain difference. Some discrepancy between obtained and applied values could arise because the proposed theory assumes material isotropy.



**Figure 14:** Two mutually perpendicular sensors,  $C_{\perp}$  and  $C_{\parallel}$  form a bridge circuit. The offset voltage,  $V_{offset}$ , is subtracted from the output signal,  $V_{out}$ , and the product is normalized by the coefficient,  $K$ .

The linear elastic limit for the polycarbonate specimen is estimated to be 3 % strain. (a) Dielectrostriction/strain response is compared with the stress/strain curve. (b) The same data are presented as the stress-dielectric response.

Actual principal-strain direction (deg)	0	10	20
Measured principal-strain direction (deg)	1.58	7.48	14.87
Measured value of $(u_1 - u_2)$	0.43-0.49 %	0.36-0.41 %	0.33-0.37 %
Actual value of $(u_1 - u_2)$	0.47-0.51 %		

**Table 2:** Comparison between measured and actual values for the principal-strain difference and the principal-strain direction.

Another preliminary study demonstrates the potential use of dielectrostriction measurements for non-destructive monitoring of the fatigue behavior under cyclic loading, Figure 15. In this case the dielectrostriction response changes significantly when cracks develop in the material.

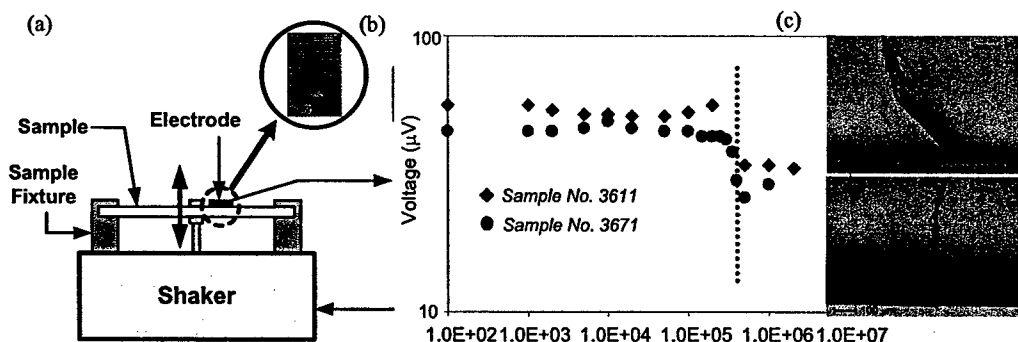


Figure 15: (a) Schematic diagram of a polycarbonate sample subjected to oscillatory bending. (b) After approximately  $5 \times 10^5$  cycles the dielectrostriction response drops dramatically. (c) Optical microscopy confirms development of multiple micro-cracks.

## CONCLUSION

Our results demonstrate the ability of FAiMTa technology to modify composites consisting of ceramic, graphite or glass-fiber inclusions in epoxy. All three systems are traditionally employed for Air Force applications. Ceramic and glass are good dielectric insulators having dielectric constants lower than epoxy. Conversely, graphite is a well-conducting material having a dielectric constant higher than epoxy. Results show that polymeric composites of various constituents, regardless of their conductivity, can be engineered and micro-tailored to fulfill desired objectives. Field-aided micro-tailoring technology is able to locally manipulate micro- or nano-sized inclusions in a polymeric matrix to enhance composite performance and optimize functionally graded materials. Our data illustrates that polymeric components can be modified up to 25 mm in depth with voltage sources and processing times which are readily acceptable for industrial processing. Such ability to control the orthotropy of composites enables one to locally modifying mechanical properties of materials. Compatible with results of our computational prediction, locally controlling the material properties in the neighborhood of a geometrical discontinuity will enable one to reduce associated stress concentrations. These results are needed for the next step in developing field-aided technology – optimization of material structure for a given design objective. The current effort focuses on orienting the particulates in a geometrically favorable manner to reduce a stress concentration. This manufacturing advancement is currently being synergized with a numerical optimization analysis to minimize the tensile stress concentration associated with geometric discontinuities in composite members.

This study also demonstrates a new approach to record strains in engineering parts through the dielectrostriction effect. In addition, the dielectrostriction enables measurements of the principal-strain difference and the principal-strain direction. Two sensor configurations were used. Experimental results demonstrate the ability to evaluate the principal-strain difference, and the direction of the principal strain in dielectric materials. However, at this stage, the dielectrostriction phenomenon is not fully understood and warrants further investigation. Following the existing analogy between photoelastic and dielectrostriction effects,



photoelasticity also provides the principal-strain difference and direction of the principal strain. However, while optical measurements are limited to optically transparent materials, dielectrostriction is applicable to transparent or opaque materials.

## REFERENCES

1. Shkel, Y.M., G.H. Kim, and R.E. Rowlands. *Analysis of graded composites fabricated by field-aided self-assembly techniques*. in *International Symposium on Experimental Mechanics*. 2002. Taipei, Taiwan.
2. Kim, G.H., Y.M. Shkel, and R.E. Rowlands, *Field-aided micro-tailoring of polymeric nanocomposites*, in *Smart Structures and Materials 2003: Electroactive Polymer Actuators and Devices (EAPAD)*, Y. Bar-Cohen, Editor. 2003, Proceedings of SPIE: San Diego, CA. p. 442-452.
3. Kim, G.H. and Y.M. Shkel, *Polymeric composites tailored by electric field*. J. Mater Res, 2004. 19(4): p. 1164-1174.
4. Kim, G.H., D.K. Moeller, and Y.M. Shkel, *Functionally Graded Polymeric Composites with Structure Micro-Tailored by Electric Field*. Journal of Composite Materials, 2004(In print).
5. Young, W.C., *Roark's Formulas for Stress and Strain*. 1989, New York: McGraw-Hill.
6. Dhir, S.D., *Optimization of opening in plates under plane stress*. AIAA journal, 1983. 21: p. 1444-1448.
7. Hermanson, J., *A finite element analysis of the influenced of curvilinear orthotropy on the state of stress in a plate with a hole* 1992, Univ of Washington.
8. Hyer, M.W. and H.H. Lee, *The use of curvilinear fiber format to improve buckling resistance of composite plates with central circular holes*. Composite structures, 1991. 18: p. 239-261.
9. Katz, Y., R.T. Haftka, and E. Altus, *Optimization of fiber directions for increasing the failure load of a plate with a hole*, in *Technical Report NAG-1-224*, NASA p. 62-71.
10. Hyer, M.W. and R.F. Charette, *Inovative design of composite structures: use of curvilinear fiber format to improve structural efficiency*, in *Technical Report 87-5*. 1987, Univ of Maryland.
11. Cho, H.K. and R.E. Rowlands, *Fiber direction optimization of a perforated orthotropic plate to reduce stress concentration around hole*. To be submitted for publication.
12. Shkel, Y.M., *Solid-State Strain Sensor and Method of Manufacture*. 2005: US Patent.
13. Filanc-Bowen, T.R., G.H. Kim, and Y.M. Shkel, *Novel sensor technology for shear and normal strain detection with generalized electrostriction*, in *IEEE International Conference on Sensors*. 2002, Proceedings of IEEE Sensors 2002: Orlando, Florida. p. 1648-1653.
14. Filanc-Bowen, T.R., G.H. Kim, and Y.M. Shkel, *Shear and normal strain sensing with electroactive polymer composites*, in *Smart Structures and Materials 2003: Smart Sensor Technology and Measurement Systems*, D. Inaudi and E. Udd, Editors. 2003, Proceedings of SPIE: San Diego, CA. p. 218-228.
15. Kim, G.H. and Y.M. Shkel, *Sensing shear strains with electrostriction effect in solid electrorheological composites*. J. Intel. Mat. Syst. Str., 2002. 13: p. 479-483.
16. Landau, L.D., E.M. Lifshitz, and L.P. Pitaevskii, *Electrodynamics of Continuous Media*. 2nd ed. Course of Theoretical Physics. Vol. 8. 1984, Oxford: Butterworth-Heinenann. 460.
17. Lee, H.Y., D.K. Moeller, and Y.M. Shkel, *Micro-tailoring composites for a self-sensing application*, in *Proceddings of the ICEM12 - 12th International Conference on Experimental Mechanics*, C. Pappalettere, Editor. 2004, McGraw-Hill: Politecnico di Bari, Italy.
18. Lee, H.Y., Y. Peng, and Y.M. Shkel, *Strain-dielectric Response of Dielectrics as Foundation for Electrostriction Stresses*. J. Appl. Phys., 2005. 98(7): p. 074104.
19. Lee, H.Y., Y. Peng, and Y.M. Shkel, *Monitoring liquid and solid polymers through electroactive response*, in *Smart Structures and Materials 2005: Sensors and Smart Structures Technologies for Civil, Mechanical, and Aerospace Systems*, M. Tomizuka, Editor. 2005, Proceedings of SPIE: San Diego, CA. p. 120-129.
20. Lee, H.Y. and Y.M. Shkel, *The dielectrostriction effect for NDE of polymeric materials*, in *Smart Structures and Materials 2004: Sensors and Smart Structures Technologies for Civil, Mechanical, and Aerospace Systems*, S.-C. Liu, Editor. 2004, Proceedings of SPIE: San Diego, CA. p. 211-218.
21. Lee, H.Y. and Y.M. Shkel. *Sensing Strains and Stresses through Dielectrostriction Response*. in *IEEE SENSORS 2005: the 4th IEEE conference on sensors*. 2005. Hyatt Regency Irvine, Irvine, California, USA.

22. Shkel, Y.M. and N.J. Ferrier, *Electrostriction enhancement of solid-state capacitance sensing*. IEEE-ASME T Mech., 2003. 8(3): p. 318-325.
23. Shkel, Y.M. and D.J. Klingenberg, *Material parameters for electrostriction*. J. Appl. Phys., 1996. 80(8): p. 4566-4572.
24. Shkel, Y.M. and D.J. Klingenberg, *Electrostriction of polarizable materials: Comparison of models with experimental data*. J. Appl. Phys., 1998. 83(12): p. 7834-7843.
25. Shkel, Y.M. and D.J. Klingenberg, *A continuum approach to electrorheology*. J. Rheol., 1999. 43: p. 1307-1322.

## **APPENDIX**

### **Personnel Supported:**

#### **Faculty:**

PI Yuri M. Shkel, Co-PI: Robert Rowlands

#### **Graduate Students**

- Yiyan Peng (Doctoral Student)
- Daniel K Moeller (Master/Doctoral Student)
- Ho Young Lee (Doctoral Student)
- Keun Cho (Doctoral Student)
- Jared A Rud (MS Student)
- John K Edmiston (MS Student)

#### **Undergraduate Students**

- Jeffrey P. Davidson (Mechanical Engineering undergraduate student)
- Kory L. Derenne (Mechanical Engineering undergraduate student)
- Christopher J. Bayliss (Mechanical Engineering undergraduate student)
- Michael W. Sracic (Engineering Mechanics and Astronomy undergraduate student)
- Joseph A. McMahon (Electrical and Computer Engineering undergraduate student)
- Shannon Cobb (Mechanical Engineering undergraduate student)
- Vladlen David Zvenyach (Mechanical Engineering undergraduate student)

## ***Publications***

### **Peer-reviewed publications**

1. Lee, H.Y., Y. Peng, and Y.M. Shkel, Strain-Dielectric Response of Dielectrics as Foundation for Electrostriction Stresses, J. Appl. Phys., 98, 15 October, 2005.
2. Y. Peng, Y. M. Shkel and G.H. Kim, Stress Dielectric Response in Liquid Polymers, J. Rheol. 49(1), pp. 297-311, January/February 2005.

### **Participation/presentations at meetings, conferences and seminars**

- 1 H. Y. Lee, Y. M. Shkel, "Sensing Strains and Stresses through Dielectrostriction Response," IEEE Sensors 2005, Nov 1-4, 2005 Irvine, CA, USA.
- 2 Y. Peng, J. K. Edmiston and Y. M. Shkel, "Dielectrostriction and Piezoresistance Response in Liquid Polymers" Proceedings of IMECE2005, 2005 ASME International Mechanical Engineering Congress and Exposition, November 5-11, 2005, Orlando, Florida USA.
- 3 H.K. Cho and R.E. Rowlands "Minimizing Stress Concentrations In Laminated Composites By Genetic Algorithm" Proceedings of IMECE2005, 2005 ASME International Mechanical Engineering Congress and Exposition, November 5-11, 2005, Orlando, Florida USA.
- 4 J. Rhee, H.K. Cho, D.J. Marr and R.E. Rowlands "On Reducing Stress Concentrations in Composites by Controlling Local Structural Stiffness" Proceedings, 2005 Conf on Experimental & Applied Mechanics, Portland, OR., June 7-10, 2005, pp. 193-199
- 5 J. Rhee, H.K. Cho, D.J. Marr and R.E. Rowlands "On Stress Concentrations and Strength in Composites" Proceedings, CANCOM 2005, Vancouver, Canada, August 11-19, 2005
- 6 Daniel K. Moeller, Hee K. Cho, Kory L. Derenne, and Yuri M. Shkel, "Micro-tailoring micro and nano composites toward variable orthotropy for biomimicking applications," Proceedings SPIE 11th Annual International Symposium on Smart Structures and Materials, 6-10 March 2005, San Diego, CA, Vol. # 5764.  
(Proceedings of SPIE -- Volume 5764 Smart Structures and Materials 2005: Smart Structures and Integrated Systems, Alison B. Flatau, Editor, May 2005, pp. 50-56)
- 7 Yiyang Peng, Ho Young Lee and Yuri M. Shkel, "Monitoring liquid and solid polymers through electroactive response," Proceedings SPIE 11th Annual International Symposium on Smart Structures and Materials, 6-10 March 2005, San Diego, CA, Vol. # 5765.  
(Proceedings of SPIE -- Volume 5765 Smart Structures and Materials 2005: Sensors and Smart Structures Technologies for Civil, Mechanical, and Aerospace Systems, Masayoshi Tomizuka, Editor, May 2005, pp. 120-129)

8      Ho Young Lee, Daniel K. Moeller, Yuri M. Shkel, "Micro-Tailoring Composites for Self-Sensing Application," ICEM12: International Conference on Experimental Mechanics, Politecnico di Bari, Italy, 29 August - 2 September, 2004.

9      Daniel K. Moeller, Yuri M. Shkel, Robert E. Rowlands, "Micro Tailoring of Nano-Composites to Reduce Stress Concentrations Associated with Geometric Discontinuities," ICEM12: International Conference on Experimental Mechanics, Politecnico di Bari, Italy, 29 August - 2 September, 2004.